Katsuyoshi Hikichi, Izumi Watanabe, Tomohiro Shinagawa, Masahito Kudo,
Toyota Motor Corporation, Toyota, Japan:

The New Toyota Inline 4 Cylinder 1.2L ESTEC D-4T Engine
Der neue Toyota 1.2L ESTEC D-4T Reihen-4-Zylinder-Motor

Abstract

Toyota Motor Corporation is developing a series of engines belonging to its ESTEC (Economy with Superior Thermal Efficient Combustion) development concept. Subsequent to the launch of the 2.0-liter DI Turbocharged 8AR-FTS, this paper describes the development of the 8NR-FTS, a 1.2-liter inline 4-cylinder spark ignition downsized turbocharged direct injection (DI) gasoline engine. Following the same basic concepts as the 8AR-FTS engine [1], the 8NR-FTS incorporates various fuel efficient technologies such as a cylinder head with an integrated exhaust manifold, the Atkinson cycle using a centre-spooled variable valve timing with mid-position lock system (VVT-iW), and intensified in-cylinder turbulence to achieve high-speed combustion. Instead of the D-4ST system that incorporates port and direct injection, the 8NR-FTS emphasizes compactness by adopting the D-4T system that performs only DI in each cylinder. In combination with a single-scroll turbocharger, high torque is achieved from low engine speeds by cooperative control with the VVT system. This engine also adopts a stop and start control strategy that achieves speedy and shock-free re-start performance by starting the engine with stratified injection in the first compressed cylinder. The engine can be mated with either a 6-speed manual transmission (6MT) or continuously variable transmission (CVT). Especially with the CVT, turbocharger lag duration is reduced by shifting control, and both fun-to-drive dynamic performance and excellent fuel economy of 10% better than a naturally aspirated (NA) 1.8-liter engine can be realized by switching between normal and sport driving modes.

Kurzfassung

Toyota Motor Corporation entwickelt neue Motoren im Rahmen des ESTEC (Economy with Superior Thermal Efficient Combustion) Konzeptes. Nach der Markteinführung des 2.0L 8AR-FTS Motors wurde mit dem 8NR-FTS Motor ein aufgeladener 1.2L Reihen-4-Zylinder-Benzinmotor mit Direkteinspritzung (DI) entwickelt. Basierend auf dem gleichen Konzept wie der 8AR-FTS Motor [1] beinhaltet der 8NR-FTS Motor zahlreiche Technologien zur Verbrauchssenkung, z.B. einen im Zylinderkopf integrierten Abgaskrümmer, den Einsatz des Atkinsonzyklus durch variable Ventilsteuerung mit Mittelpositionsfixierung (VVT-iW) und erhöhte Turbulenz im Zylinder für schnellere Verbrennung. Während das D-4ST System auch Kanaleinspritzung beinhaltet, fokussiert der 8NR-FTS Motor auf Kompaktheit und setzt das D-4T System als reines DI-System ein. In Kombination mit einem single-scroll Turbolader und durch entsprechende VVT-Steuerung kann hohes Drehmoment bereits bei niedrigen Drehzahlen erreicht werden. Die Motorsteuerung nutzt eine Stop&Start Strategie für das rasche und schockfreie Wiederstarten durch geschichtete Ladung im ersten Verdichtungszyklus. Der Motor kann entweder mit einem 6-Gangschaltgetriebe (6MT) oder einem kontinuierlich variablen Getriebe (CVT) kombiniert werden. Das CVT-Getriebe erlaubt es, das Ansprechverhalten des Turboladers durch entsprechende Getriebesteuerung weiter zu verbessern. Durch

diese Massnahmen können sowohl die zum Fahrspass beitragende transiente Fahrzeugbeschleunigung als auch der Verbrauch im Vergleich zum 1.8L Saugmotor (NA) in den jeweils vorteilshaften Normal- bzw. Sportmodi um etwa 10% verbessert werden.

1. Introduction

Following the launch of the 2.0-liter DI Turbocharged 8AR-FTS(ESTEC) engine, Toyota Motor Corporation has developed the new 1.2-liter 8NR-FTS(ESTEC), an inline 4-cylinder downsized turbocharged direct injection (DI) gasoline engine. This engine is due to be launched in Japan in March 2015 and in Europe in May 2015 as a partial replacement for existing 1.6-liter to 1.8-liter naturally aspirated (NA) engines. Table 1 shows the main differences between the new 8NR-FTS engine and the previously launched 8AR-FTS engine. The new engine incorporates a single-scroll turbocharger manufactured by IHI Turbo Co., Ltd. and is Toyota's first new DI engine without port injection for 12 years since the 3GR/4GR-FSE engines developed in 2003. The engine can be mated with either a 6-speed manual transmission (6MT) or continuously variable transmission (CVT).

Table 1. Comparison of 8NR-FTS and 8AR-FTS

	8NR-FTS (ESTEC D-4T)	8AR-FTS (ESTEC D-4ST)
Displacement	1.2-liter	2.0-liter
Injection system	DI	DI + PFI
Turbocharger	Single-scroll	Twin-scroll
Turbocharger Manufacturer	IHI	Toyota
Transmission	6-speed MT 7-speed CVT	6-speed AT

2. Engine Specifications and Combustion Concepts

Table 2 shows the main specifications of the engine. The 8NR-FTS is part of Toyota's ESTEC series of engines (ESTEC is the name of Toyota's next-generation engine technology and stands for "Economy with Superior Thermal Efficient Combustion"). The engine has a compression ratio of 10, uses fuel with a research octane number (RON) of 95 or above, and is compliant with the Euro 6 and J-SULEV emissions regulations.

The fundamental approach of these engines is to achieve high-speed combustion through high intake flow and intense in-cylinder turbulence. The 8NR-FTS is Toyota's lowest displacement DI engine and has a relatively small bore diameter. Consequently, a more intense intake flow than a conventional engine is necessary for mixing the injected fuel with air before the fuel spray contacts the cylinder bore. Therefore, to enhance the flexibility of intake port shape design and ensure mountability, this engine adopted a simple DI approach without port injection. As shown in Fig. 1, this approach allowed the port shape to be optimized to intensify the intake flow and in-cylinder tumble. In addition, the conventional shallow cavity piston was changed to a dog dish type curved piston to achieve stable combustion with a retarded spark timing in the process for rapid catalyst light-off, without restricting in-cylinder tumble (Fig. 2) [2]. These measures prevent the attenuation of tumble and intensify in-cylinder turbulence in the latter phase of the compression stroke (Fig. 3).

Table 2. Engine specifications

Displacement (cc)	1,197
Bore x stroke (mm)	ϕ71.5 x 74.5 (S/B=1.04)
Compression ratio	10.0
Injection system	D-4T
Spray shape	Fan spray
Intercooler	Water-cooled
Max. power (kW/rpm)	85/5,200 to 5,600
Max. torque (Nm/rpm)	185/1,500 to 4,000
Fuel	95 RON
Emissions	Euro 6, J-SULEV

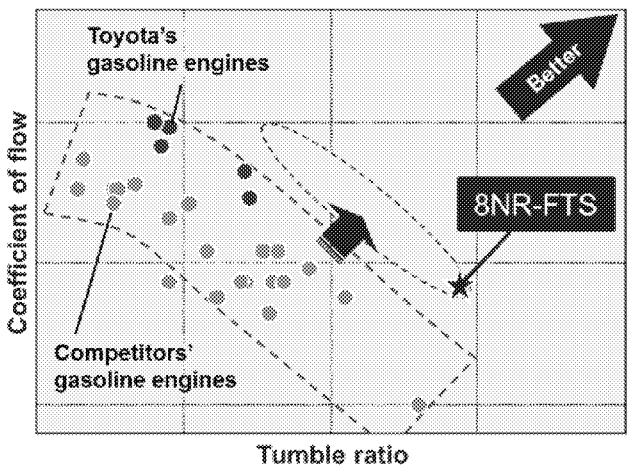

Figure 1. Flow coefficient and tumble ratio

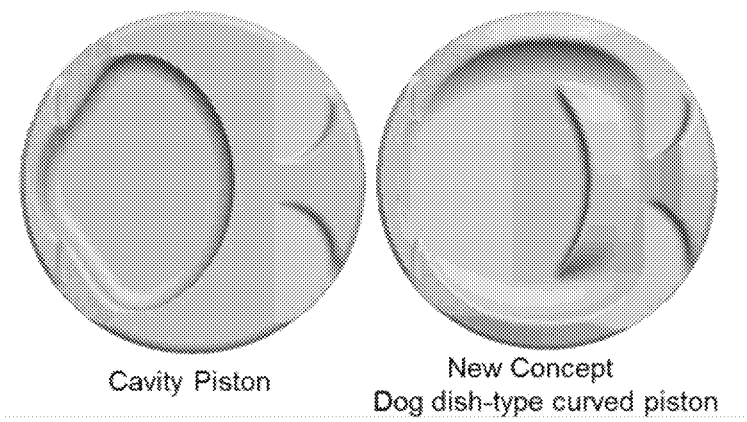

Figure 2. Comparison of piston shapes

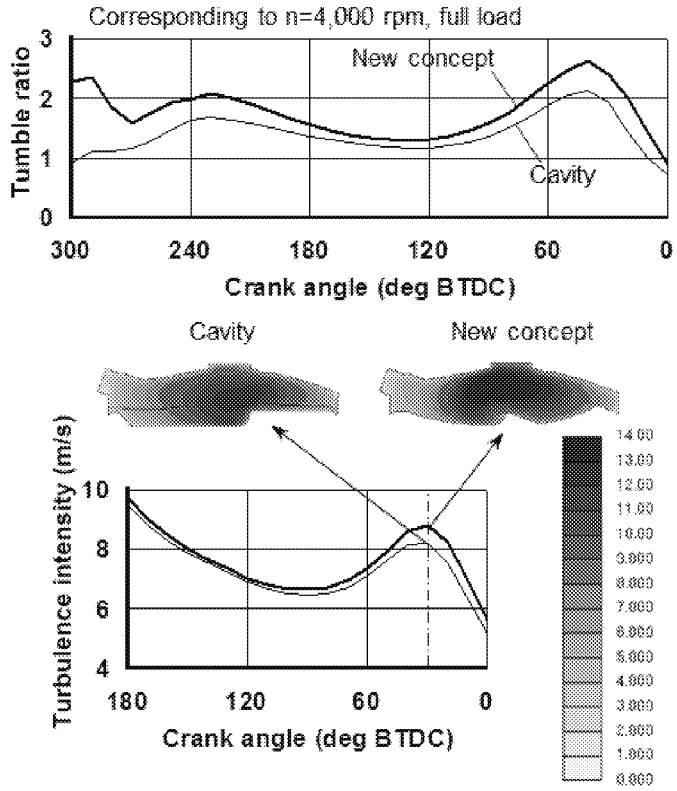

Figure 3. Comparison of unsteady tumble ratio and turbulence intensity

This engine utilizes the same fan spray as Toyota's other DI engines. However, to prevent fuel spray wetting on the bore wall, the thickness of the slit and the fuel film have been made narrower (Fig. 4). This increases the shearing force between the fuel and air, promotes atomization, and reduces the length of the spray by 23% compared to the conventional fan spray. In addition, to reduce fuel contact on the intake valve (Fig. 5), the valve included angle and injection angle were optimized, and the length of the spray of each injection within multiple injections in a single combustion cycle was shortened (see below for more details). These measures improved the air/fuel (A/F) mixture and reduced fuel wetting on the bore wall (Fig. 6). In addition, the oil separation function of the positive crankcase ventilation (PCV) function was enhanced to thoroughly reduce the amount of oil entering the intake system. This helps to reduce the amount of deposits in the intake system, which is a common issue of DI engines.

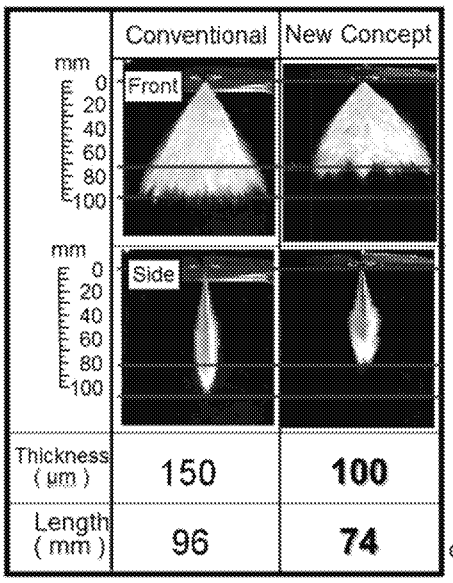

Figure 4. Comparison of fan sprays

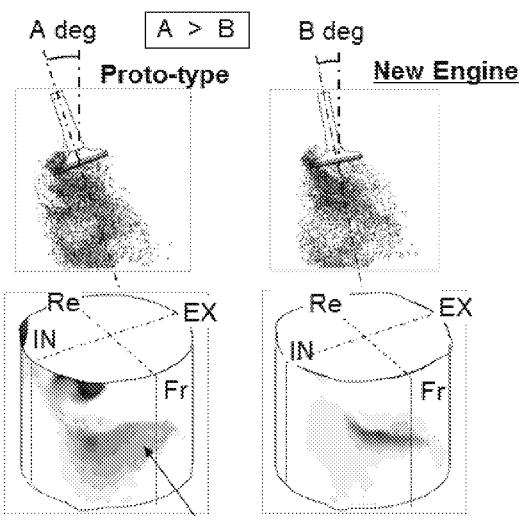

Fuel on bore wall due to scattering by intake valve contact

Figure 5. Comparison of fuel wetting on cylinder bore wall

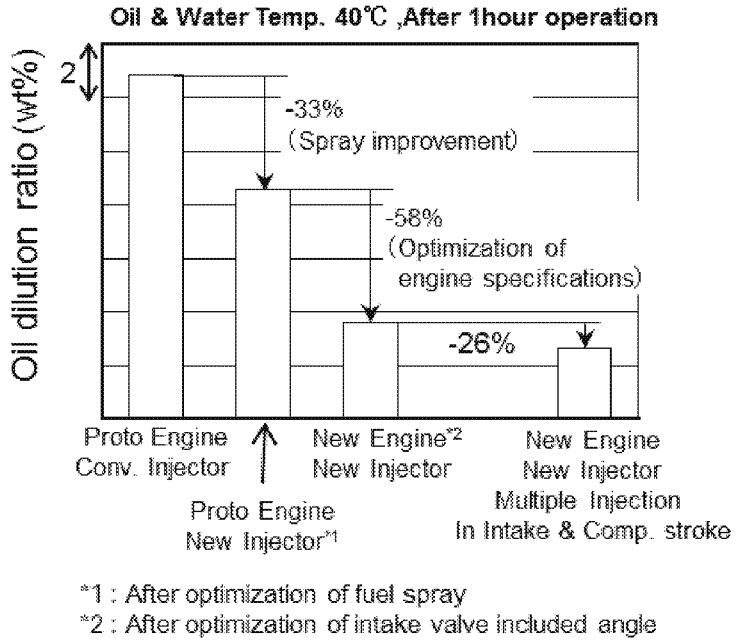

Figure 6. Dilution ratio of fuel in oil

3. Turbocharger and Exhaust System

In the exhaust system, the exhaust manifold is integrated into the cylinder head. This reduces the overall size of the engine and helps to achieve a smoother exhaust flow pattern (Fig. 7). It also optimizes the change in port sectional area and reduces the exhaust area. In addition, the catalyst is also located immediately downstream of the turbocharger to reduce the distance to the catalyst and to improve cold start catalytic performance (Fig. 8).

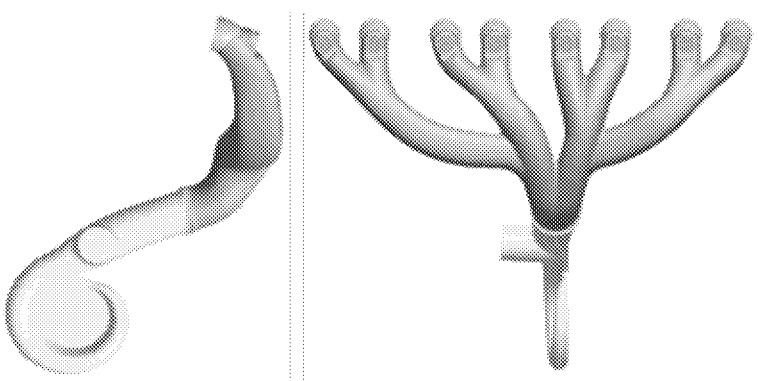

Figure 7. Exhaust port geometry

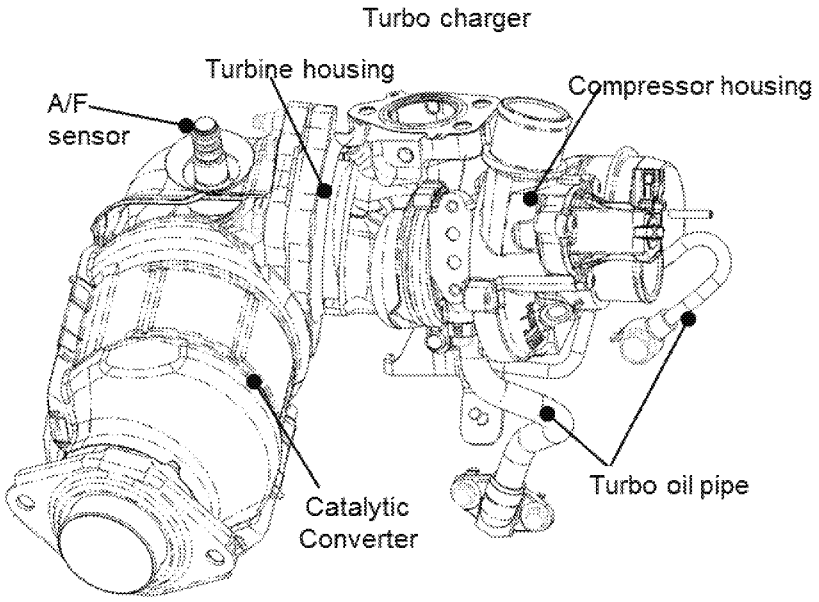

Figure 8. Turbocharger and catalytic converter arrangement

On the turbine side, to ensure both torque at extremely low engine speeds (i.e., low-end torque) and transient response performance, a low-inertia single-scroll turbocharger was adopted with high efficiency over a wider range of turbine speeds. In addition, an active wastegate system was adopted that enables flexible control over the degree of wastegate valve (WGV) opening. When the engine is started, the WGV is opened to supply high-temperature gas to the catalyst, thereby reducing the catalyst light-off time. The WGV is also opened in low engine load operating regions to reduce exhaust losses. This increases fuel economy by lowering pumping loss and improving combustion characteristics by decreasing the amount of residual gas.
Thoroughly reducing the back pressure for the whole exhaust system enabled higher performance and response.
In addition, a water-cooled turbocharger was applied to reduce heat soak-back immediately after dead soak start, restrict the generation of oil coking, and enable the turbocharger to be used with a stop and start system. Furthermore, with specific focus on the turbine housing, the entire exhaust system was subjected to thermal stress analysis and durability testing to ensure compatibility with the high temperatures likely to be generated by an engine backside exhaust system, as well as the higher gas temperatures. As a result of this analysis and testing, the shapes and materials were optimized to ensure high heat resistance.

3.1. Air-Fuel Ratio Sensor Installation Position and Flow Passage Shape

The shapes of the flow passages around the air-fuel ratio (A/F) sensor were specially designed to allow precise sensing of the A/F ratio under virtually any WGV opening angle, bypass ratio, and airflow conditions. In particular, when the WGV is open, the shapes are designed to actively guide only the gas from the WGV to the sensor. This enables precise A/F sensing for each cylinder by facilitating contact between the sensor and gas that has not been agitated by the turbine. The positions of the wall surfaces and sensor were also determined to help prevent breakage of the sensor element due to water intrusion (Fig. 9).

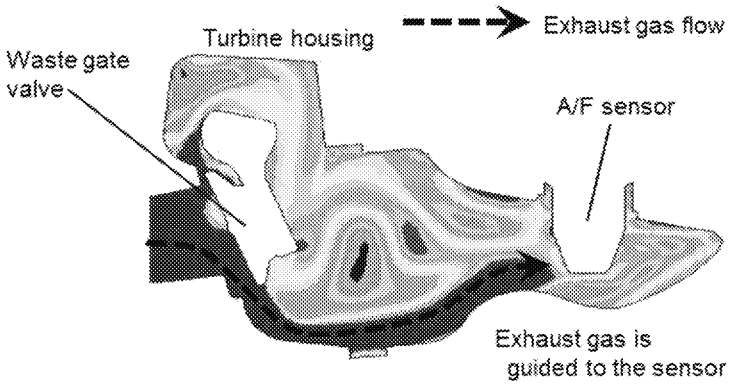

Figure 9. Exhaust gas flow around A/F sensor

4. Full Load Performance

One advantage of downsized turbocharged engines is the availability of large low-end torque. This helps to improve fuel economy since engine operating points for achieving equivalent power to a conventional engine can be set at higher geared and lower engine speed locations on the engine map. In addition, with a manual transmission, plentiful torque is available at low engine and vehicle speeds. This reduces the frequency of gear changes and eliminates wasteful increases in engine speed. As a result, the driver can achieve the intended dynamic performance with better fuel economy. The key for realizing this advantage is to secure sufficient low-end torque, and various approaches have been adopted by different companies to reduce the engine speed at which maximum torque is available [3, 4].

Generally, to increase the boost pressure, it is necessary to increase the exhaust energy flowing into the turbine (i.e., to increase the exhaust flow and the exhaust temperature). However, the smaller airflow makes it difficult to secure high boost pressures at low engine speeds. One possible countermeasure is to change the valve timing and set the intake valve closing position close to bottom dead centre (BDC). This should help to prevent intake blowback and ensure sufficient airflow. However, this measure results in a large overlap at top dead centre (TDC). In the case of an in-line 4-cylinder engine, exhaust blowback flow of the next exhaust cylinder increases the residual gas in the cylinder. Eventually, in fact, not only the amount of air is not increased, but the knocking has been caused by increasing the in-cylinder temperature (Figs. 10 and 11). In the figure.10, η_{vb} means the volumetric efficiency corrected under room temperature and atmospheric pressure conditions. This value corresponds to the volumetric efficiency at wide open throttle (WOT) and no boost.

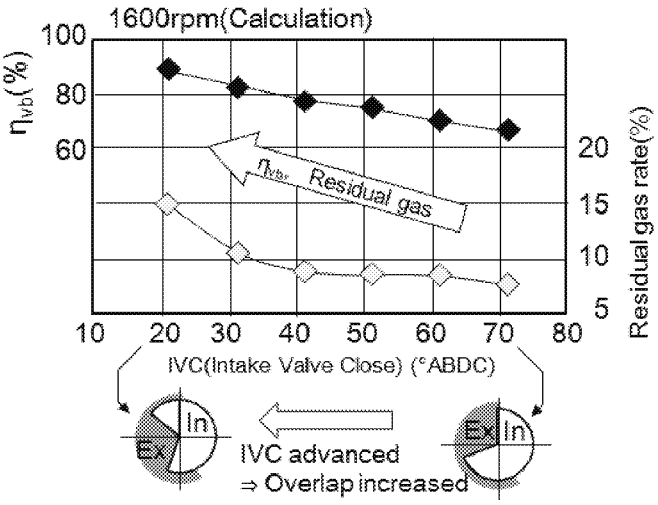

Figure 10. Relationship of valve timing with airflow and residual gas

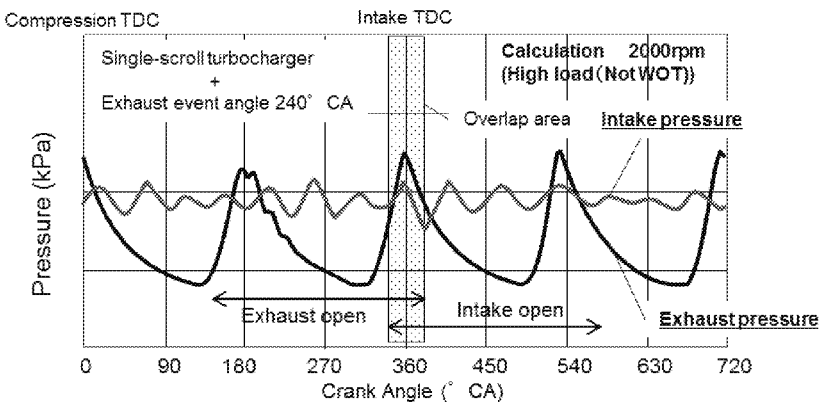

Figure 11. Pulsation of intake and exhaust pressure

To avoid this phenomenon, Toyota adopted a twin-scroll turbocharger on the 8AR-FTS engine to physically reduce the exhaust blowback flow in the next cylinder during the overlap period. However, for reasons of mountability and productivity, the current 8NR-FTS engine uses a single-scroll turbocharger. Therefore, the exhaust cam event angle was reduced to offset the timing of the overlap period and the blowback pulsation (Fig. 12). Figure 13 shows the verification results of the volumetric efficiency ηv and ηvb based on simulations and actual engine operation after changing the exhaust cam event angle. The results show that the amount of air increases when the exhaust cam event angle is reduced.

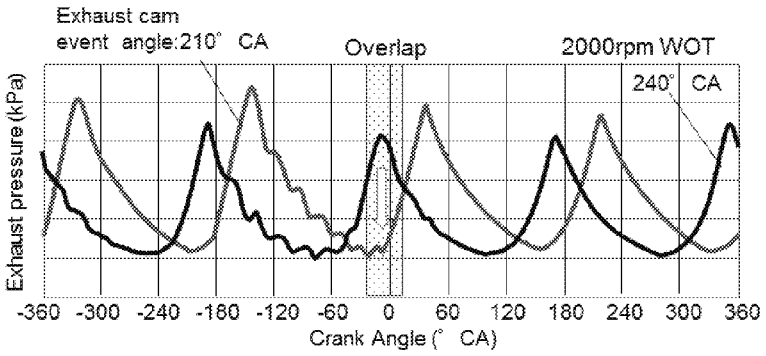

Figure 12. Effect of reducing exhaust valve event angle

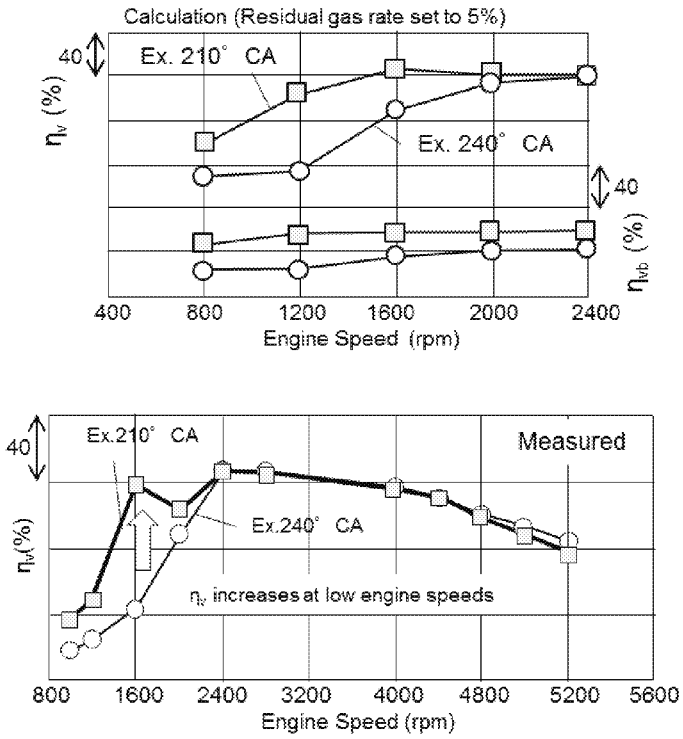

Figure 13. Changes in airflow in accordance with exhaust valve event angle (Calculated values and actual values)

One potential cause of low speed pre-ignition (LSPI) is fuel dilution in engine oil [5, 6]. To reduce the amount of fuel dilution, three injections of fuel are carried out in each intake or compression stroke (Fig. 14). Injection timings have been set to avoid the fuel contact with the intake valve and wetting on the cylinder bore wall. This measure virtually eliminates pre-ignition, reducing its frequency to a level at which no damage is caused to the piston or piston rings.

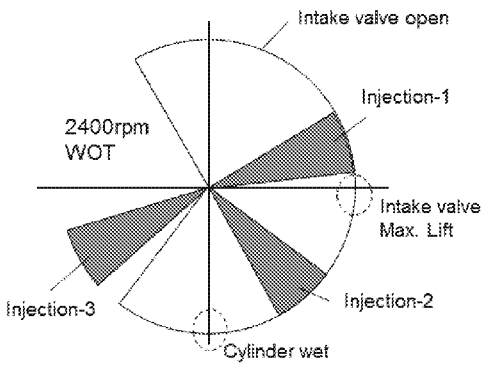

Figure 14. Injection timings to avoid LSPI

In contrast, the increase in boost pressure at high engine speeds has a trade-off effect. Knocking caused by the greater back pressure and larger amounts of residual gas causes the spark timing to be retarded, leading to higher exhaust temperatures. Consequently, due to restrictions on the turbine inlet gas temperature, the fuel injection quantity must be increased to cool the exhaust temperature. Therefore, to lower the back pressure, the thickness of the walls between the cells in the catalyst was reduced by one-third compared to a conventional catalyst. In addition, the strength of the substrate was increased which

resulted in a hexagonal catalyst shape. These measures ensured the emissions conversion performance.
Other measures included the adoption of a cylinder head with integrated exhaust manifold as shown in Fig.14, exhaust cooling, the lowering of back pressure, decreasing the residual gas and expanding the λ=1 (stoichiometric) combustion region. The cylinder head with integrated exhaust manifold has a compact design that ensures a uniform cooling capacity for each port and eliminates the effect of blowback. The cooling function is concentrated at the curved exhaust port manifold portion, thereby increasing the exhaust cooling efficiency. Longer individual exhaust ports were also designed to utilize the turbocharger efficiency to the maximum extent. In addition, when the exhaust temperature is relatively low, the amount of cooling is reduced to secure sufficient turbine performance. The integrated exhaust manifold also has the optimum cooling design for high engine loads that cause the exhaust temperature to increase. These measures help to expand the λ=1 combustion region.

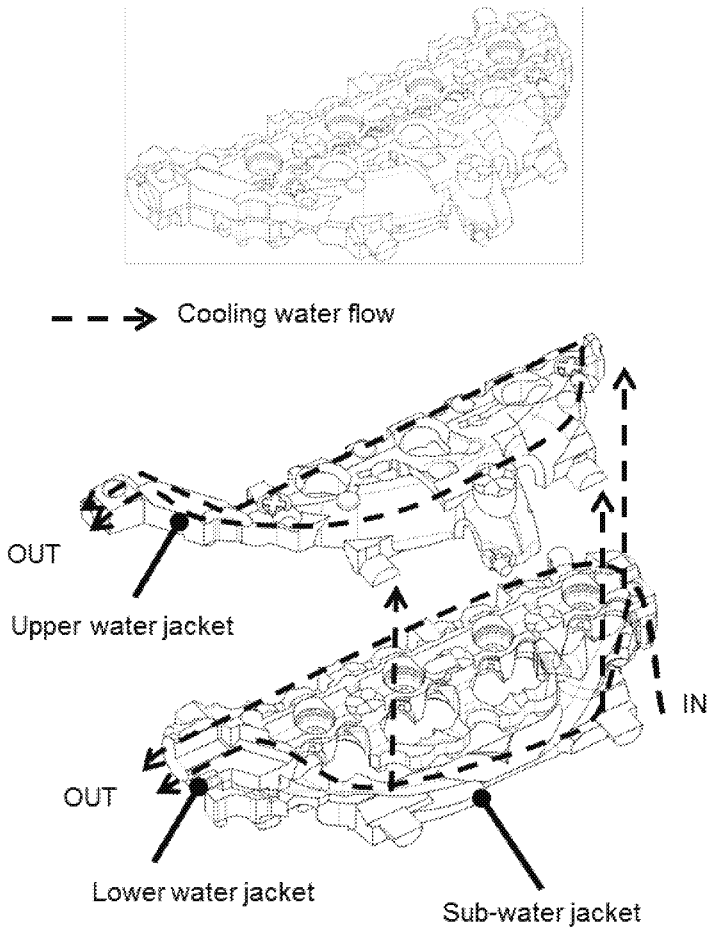

Figure 15 Water flow of cylinder head

As a result, Fig. 16 shows the full load performance. Low-end torque of 185 Nm was achieved from 1,500 rpm with a maximum power of 85 kW at λ=0.89.

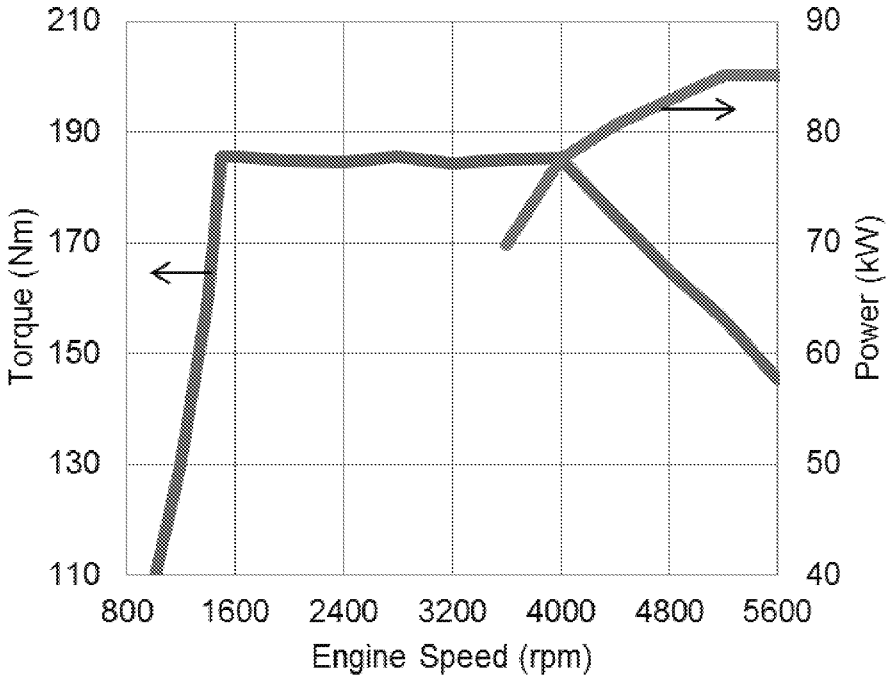

Figure 16. Full load performance

5. Fuel Consumption

5.1. Fuel Consumption of Engine

One of the main factors causing poor fuel economy is pumping loss in low load engine operating regions. To reduce pumping loss in the 8AR-FTS engine, Toyota adopted the Atkinson cycle using a centre-spooled variable valve timing with mid-position lock system (VVT-iW).

The 8NR-FTS also uses VVT-iW to improve fuel economy in low load regions. However, pumping loss cannot be reduced enough in case of only phase shift of intake side because of a negative overlap period (Fig. 17). A possible countermeasure is to increase the overlap by also shifting the exhaust valve timing. However, since this engine has a small exhaust event angle to achieve low-end torque at low engine speed, if the overlap is increased, the exhaust valve open timing is retarded beyond BDC. This increases pumping loss and worsens fuel economy. Fig.18 shows a change of the fuel consumption for the valve timing and overlap. The contour lines in this figure express aggravation charges from the best fuel economy point in percentages. When the exhaust valve open timing (EVO) is set before about 30~35 °BBDC, the fuel consumption is improved for both the overlap effects and enlargement of the expansion ratio (Line A). At the region between line A and B, only overlap improves the fuel economy. However, in the case that the EVO set after BDC for large overlap period, the fuel economy gets worse because of increasing the pumping loss at compression stroke. As a result, the fuel economy effect of the Atkinson cycle cannot be fully achieved.

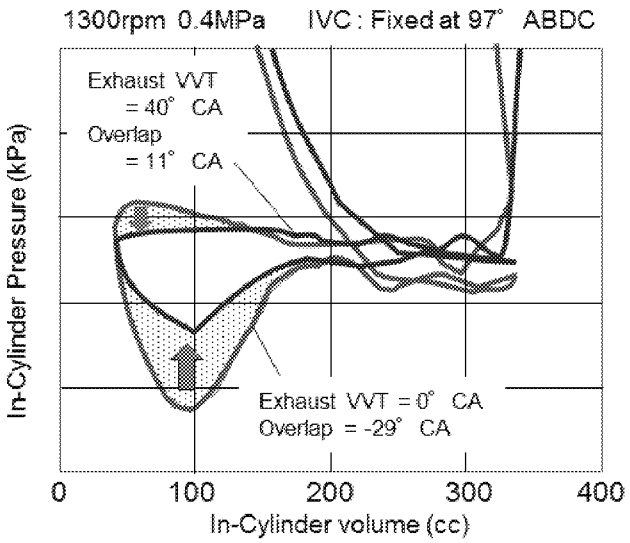

Figure 17. Effect of exhaust VVT for decreasing pumping loss

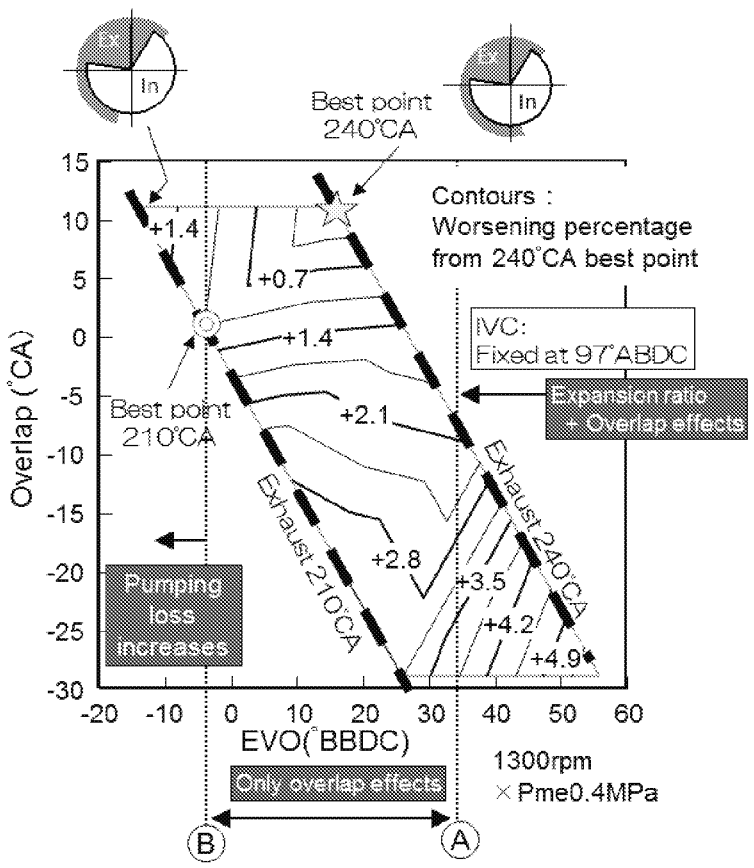

Figure 18. Effect of Atkinson cycle due to valve timing

Under medium loads, the back pressure increases in accordance with the increase in boost pressure. In other words, increasing the boost pressure creates a trade-off effect of higher pumping loss. Therefore, to improve fuel economy in this operating region, the application of boost must be minimized and sufficient airflow must be secured as a NA engine. This is accomplished by changing the intake valve timing and closing the intake valve as close as possible to BDC.

Because of these points and the continuity to full load operation, this engine limits the application of the Atkinson cycle to extremely low loads (Fig. 19). As the load increases, the intake valve closing timing is changed from late to early, thereby achieving a good fuel economy balance over the entire operating range of the engine. The VVT-iW system was adopted to increase shifting speed since the VVT settings must achieve large changes in accordance with fluctuations in the volumetric efficiency [1].

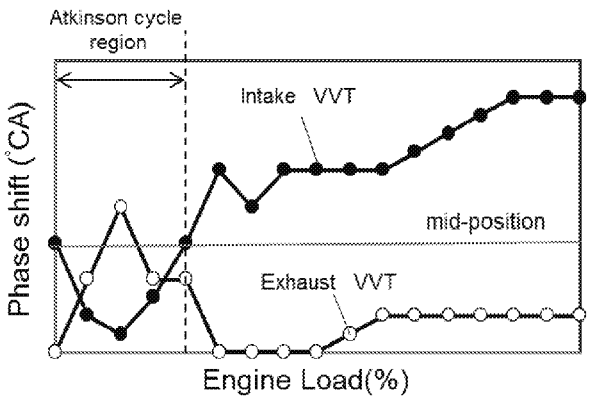

Figure 19. VVT settings

Fuel economy was also improved through combustion measures. The number of injections and injection timing in each combustion cycle were optimized in the low, medium, and high load regions. To prevent deterioration in combustion properties under low loads because of the lower temperature of the compressed gas in the Atkinson cycle, and to speed up combustion velocity at low engine speed or high loads, injection was set in the compression stroke to form a weak stratified mixture around the plug. Under medium loads, injection is carried out close to BDC, at which the intake flow velocity is attenuated to increase in-cylinder turbulence and speed up the combustion velocity (Fig. 20). These injection timings are changed during periods of warm and cold engine operation. Especially under cold conditions, the weak stratified regions have been increased to improve combustion (Fig. 21).

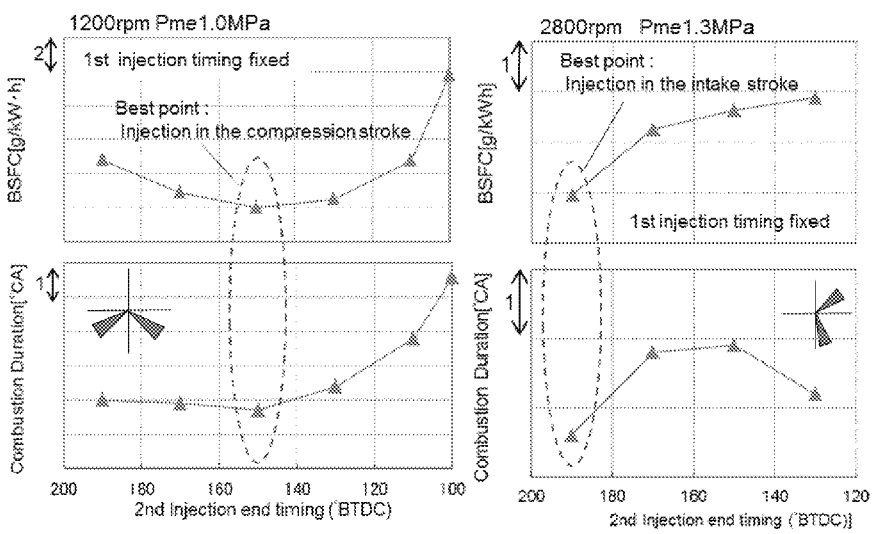

Figure 20. Improving combustion by changing injection timing

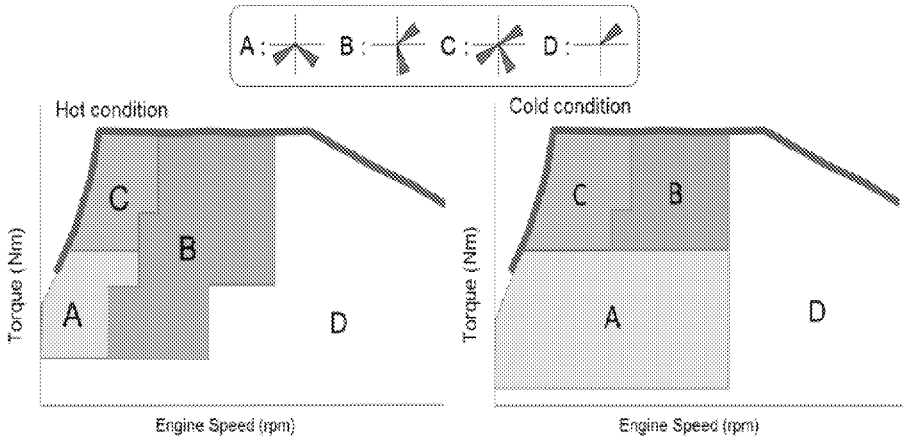

Figure 21. Hot and cold injection strategy

Mechanical losses were also thoroughly reduced. An offset crankshaft was adopted to lower piston friction loss and to improve thermal efficiency. Around both the intake and exhaust valves, the use of thinner roller arms, smaller retainers, beehive-shaped valve springs, and sodium-filled hollow exhaust valves reduced the inertial mass and the valve spring load. Other friction-reduction measures include the adoption of a low sliding resistance timing chain and low friction material chain guide, the application of fine surface reforming (FSR) to the piston skirts and a low-friction coating to the oil sealing lip of the crankshaft. Measures were also applied to the lubrication system. To minimize the discharge volume of the oil pump while ensuring sufficient hydraulic pressure and oil flow for valve train and VVT operation and for turbocharger reliability, the working parts of the hydraulic pressure system were laid out as much as possible on the upstream side. CAE was also adopted to optimize the lubrication paths and oil supply flows. Highly efficient pump teeth were also adopted that help to reduce the mechanical loss of the oil pump. In addition to a newly developed high-strength connecting rod material, lowering the reciprocating inertial mass allowed the adoption of a lighter crankshaft.
Figure 22 shows the brake specific fuel consumption (BSFC) and λ (excess air ratio) for the whole engine operating range. The minimum specific fuel consumption is 236 g/kWh (brake thermal efficiency: 36.2%). Partially due to the effects of the cylinder head with integrated exhaust manifold, the region of λ=1 combustion is expanded to a speed of 190 km/h (compared to a maximum speed of 195 km/h), enabling combustion with a stoichiometric mixture in virtually every engine operation region.

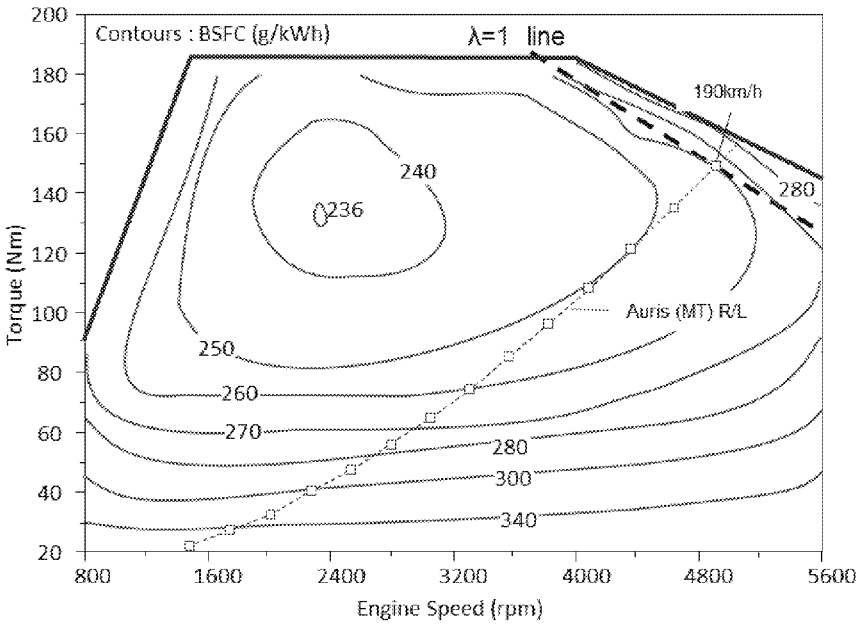

Figure 22. Brake Specific Fuel Consumption Map

5.2. Stop and Start Control Strategy

A new start control with stratified injection and combustion in the first compressed cylinder was developed for re-starting after the engine is shut down while the vehicle is stopped. This control has already been adopted in the previous 8AR-FTS engine. This system aims to re-start the engine more quickly than the conventional re-start control using port injection, and to achieve smooth re-starts by restricting engine revving.

In the same way as the conventional port injection control, the throttle is opened immediately before the engine is stopped to increase the in-cylinder air. The rebound force from the pressure of the compressed gas is used to control the piston stop position at around 90° before top dead centre (BTDC). Upon re-start, the starter is used to begin cranking and injection is carried out before TDC in the compression stroke cylinder. A combustible gas mixture is formed around the plug and retarded ignition is performed.

As shown in Fig. 23, the re-start time achieved by this injection control is approximately 200 ms faster than a conventional port injection re-start. The highly retarded ignition also has the effect of controlling the rate of torque increase, thereby restricting engine revving. As a result, lower brake hold pressure is required, enabling a shock-free re-start.

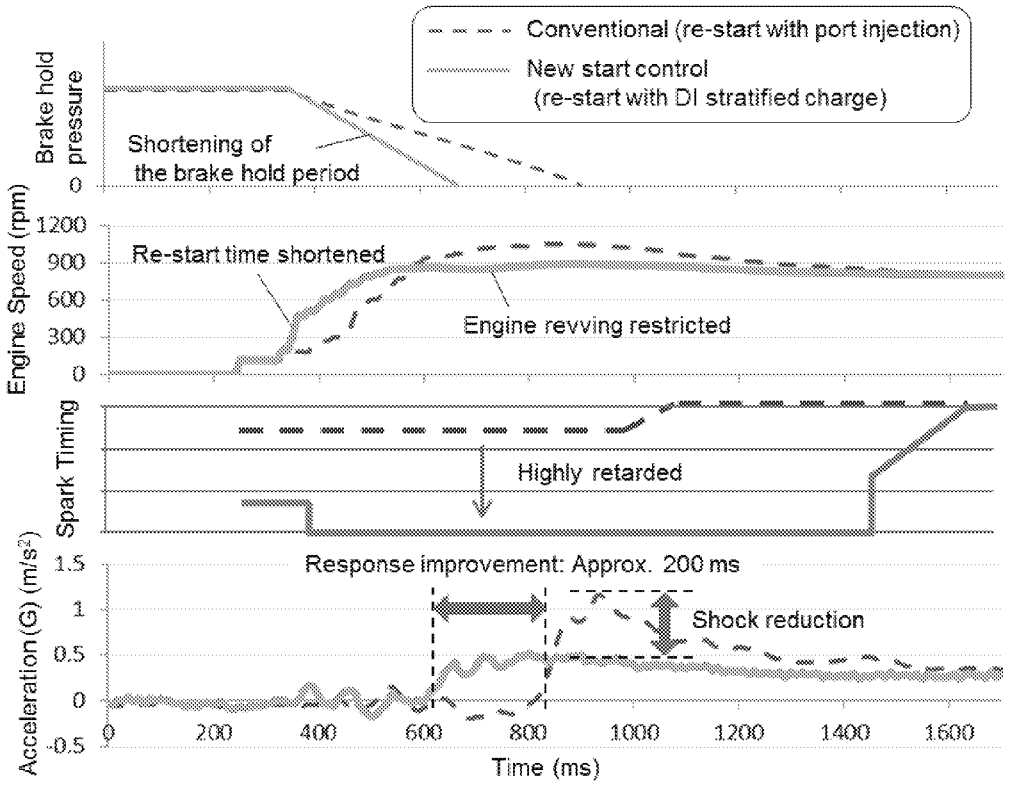

Figure 23. Re-start performance of new stop and start system

5.3. Heat Management

To improve the fuel economy of the warm up process, the amount of coolant used by the engine, CVT, and interior heater (i.e., the heat distribution) was optimized by CAE. During the warm up process, the heat distribution prioritizes the engine and heater to ensure interior comfort and improve fuel economy by reducing engine friction loss. In addition, the inside of the engine block is structured so that the oil communication passage and water jacket are in close vicinity (Fig. 24) to allow heat exchange between oil and coolant. During the warm up process, heat is transferred from the coolant to the oil, which promotes the temperature increase of each sliding part. In contrast, under high temperatures and loads, heat from the oil is transferred to the coolant, creating an oil cooler effect and eliminating the need for an oil cooler in the structure (Fig. 25).

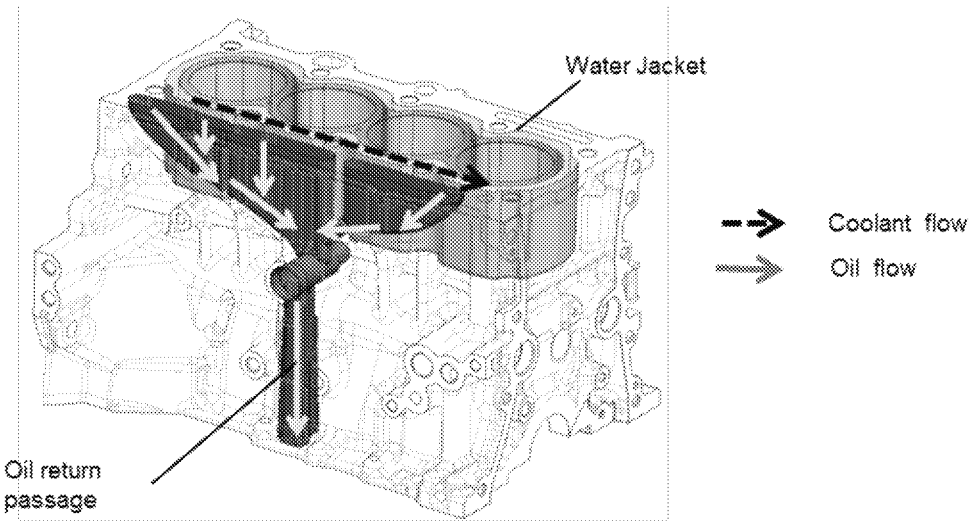

Figure 24. Structure of engine block with oil-cooling function

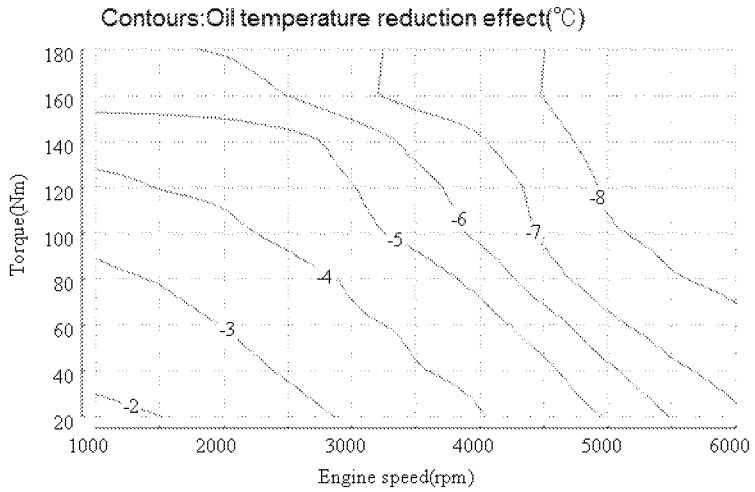

Figure 25. Oil temperature reduction effect of engine block with oil-cooling function

The new 8NR-FTS engine also uses some of the technologies adopted in the 8AR-FTS engine. These include a heat retention system that promotes the warming up of the cylinder block by reducing the coolant flow to the cylinder block under cold conditions with a block thermostat (Fig. 26), and a system that stops the piston cooling jets, which halts the supply of cooling oil to the pistons and limits excess cooling of the pistons and piston rings in accordance with the driving state to reduce sliding friction with the bore. The system that stops the piston jets is incorporated inside the cylinder block, and consists of an additional passage parallel to the high-pressure oil passage (oil gallery). This system can stop the flow of oil to the piston jets while supplying oil to the crankshaft journal at all times.

In addition, the cylinder head with integrated exhaust manifold also recovers waste heat and speeds up the increase in coolant temperature to support the temperature increase of the cylinder bore and other parts. This helps to improve fuel economy.

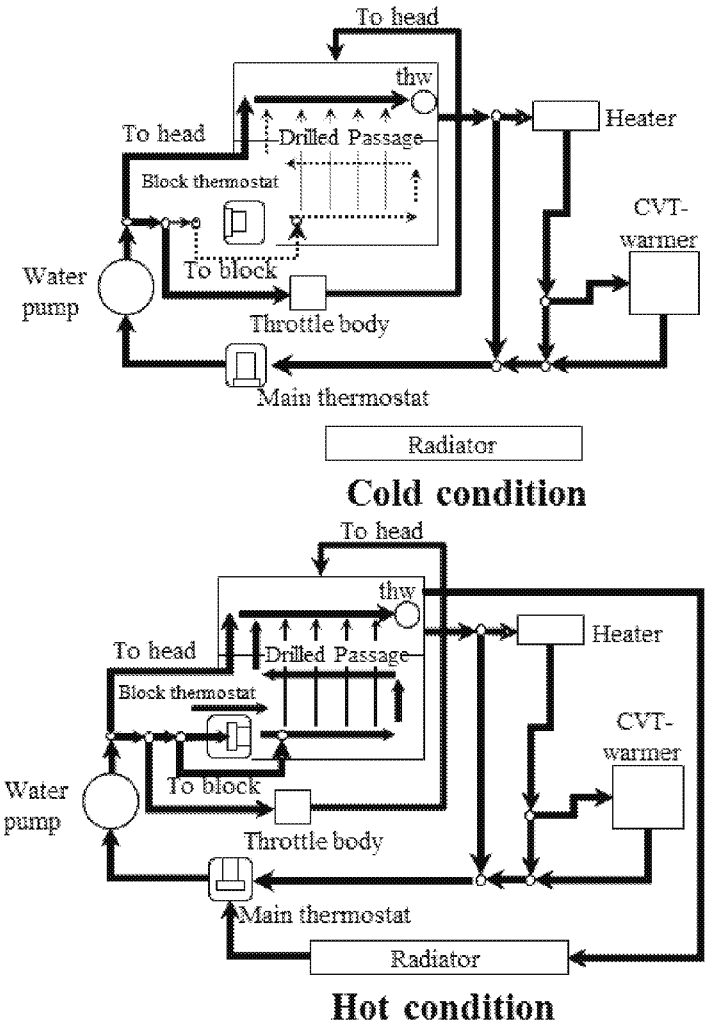

Figure 26. Cooling circuit

Due to these engine-based fuel economy improvements, enhanced stop and start control, heat management systems, the reduction in engine speed achieved by increasing low-end torque, and optimized charge/discharge control of the alternator and battery, vehicle fuel economy was improved by about 25% in the NEDC cycle, compared to the previous NA 1.8-liter engine.

6. Vehicle Dynamic Performance

6.1. Low-Speed Response

To improve the dynamic performance of the vehicle, it is important to reduce the duration of turbocharger lag as well as to improve the full load performance of the engine itself. Since a key aim of 8NR-FTS is to achieve fast transient response, the volume of the intake system was minimized and the intake pressure loss was reduced, including the intercooler. The volume of the surge tank was reduced to 1.1 litres, the lowest volume per unit of displacement for any Toyota vehicle. The intercooler system has a water-cooled design to minimize the volume of the intake system downstream of the turbocharger. The intercooler uses a low-temperature cooling circuit that is independent from the engine cooling system and includes an electric water pump. This cooling circuit controls the flow of coolant to maintain the optimum cooling effect in accordance with the engine operating state, while minimizing the power consumption of the water pump. The internal design of the

intercooler was revised to increase cooling efficiency by providing inner fins on the water passage side and optimizing the shapes of the fins and tubes on the supercharged air side (Fig. 27).

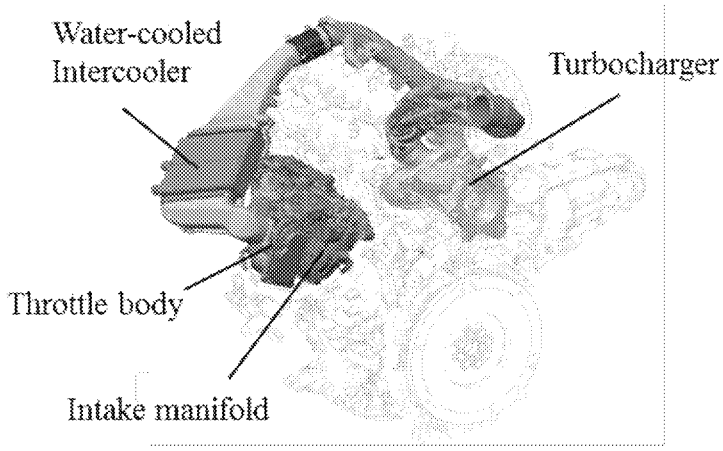

Figure 27. Intake system

The turbocharger WGV is driven by a vacuum actuator that uses the negative pressure generated by the vacuum pump as its drive source. In the event that the WGV receives intermittent opening and closing commands, a negative pressure tank is provided in the vacuum lines to ensure the rapid response of the WGV to requests of high levels of vacuum on a recurring basis.

In addition, to reduce the temperature of the intake, the intake passages use a high number of plastic parts to prevent as much heat transfer from the engine compartment as possible.

Dynamic performance is also improved by controls. In addition to the WGV control, scavenging control is carried out in which the valve overlap is temporarily enlarged compared to ordinary settings to increase the boost pressure over the back pressure. This increases the volume of gas entering the turbine and maintains the boost pressure. As shown in Fig. 28, these measures shorten the duration of turbocharger lag.

Since increasing the low end torque results in the generation of more heat at low engine speeds than an NA engine, the cooling system for low engine speeds was enhanced. In particular, if a high load is applied while the flow volume is restricted by the block thermostat, an increase in engine coolant temperature and partial evaporation of coolant are likely to occur due to reduced flow volumes. Therefore, the distribution of flow to the high temperature exhaust manifold inside the engine was optimized, and the pressure loss of the engine, piping, and all cooling devices was thoroughly reduced.

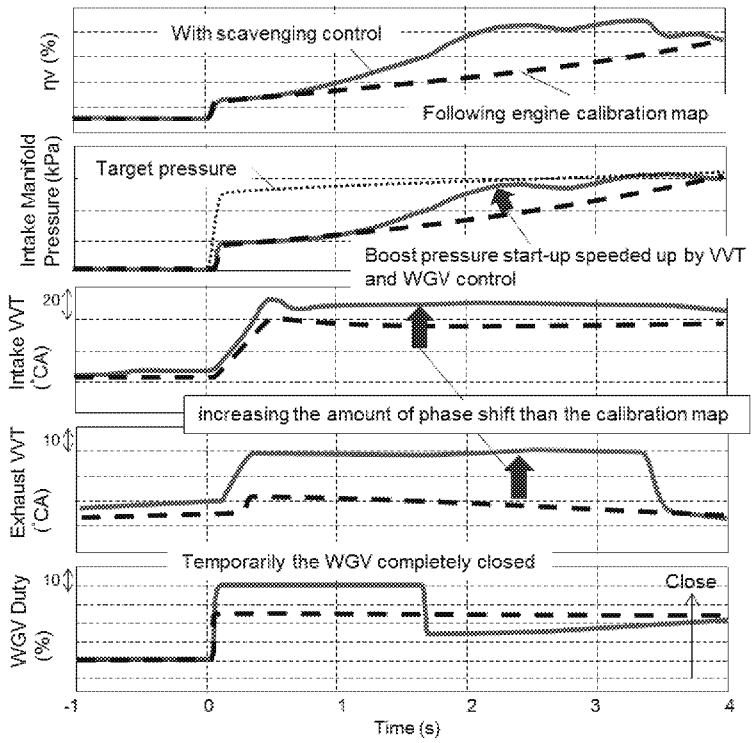

Figure 28. Scavenging control for improvement of low speed response

6.2. Engine with CVT Integration Development

One of the main features of this turbocharged engine is that it can be mated with a CVT. As a first step, this development studied ways of optimizing CVT shifting control with a turbocharged engine.

Figure 29 shows the vehicle longitudinal acceleration (G) curves for two types of shifting control under WOT acceleration from 30 km/h. Curve A shows the data when the engine speed is increased rapidly. Curve B shows the data when the increase in engine speed is restricted. Curve C is the data for a vehicle equipped with a manual transmission under the same conditions. In the case of curve A, G initially remains steady, before decelerating and then suddenly increasing. In the case of curve B, the same linear increase in G is achieved as the manual transmission vehicle.

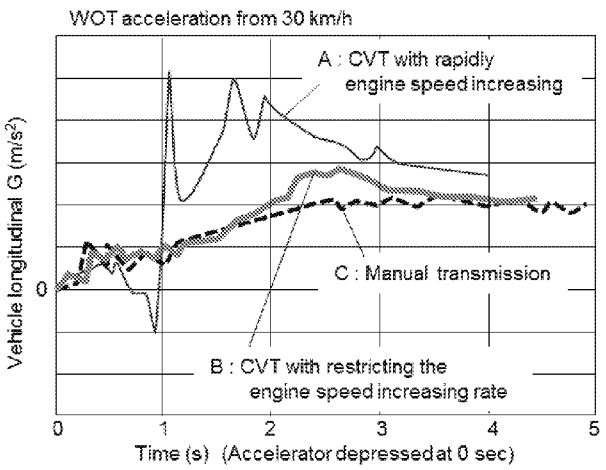

Figure 29. Differences in vehicle acceleration in accordance to shifting control

Figure 30 shows the volumetric efficiency per combustion cycle with respect to engine speed for the data shown in Fig. 29. With curve A, the volumetric efficiency shows virtually no increase up to approximately 4,000 rpm before the airflow suddenly increases. This is probably because if the engine speed is increased quickly in the same way as an NA engine, the increasing rate of the boost pressure balances with the increasing rate of the amount of intake air. As a result, the volumetric efficiency per combustion cycle does not increase. Furthermore, the increase in inertia loss accompanying the shifting causes the initial deceleration. In contrast, curve B shows a linear and responsive increase in boost pressure utilizing the highly flexible shifting control performance of a CVT to restrict the amount and rate of engine speed increase. Furthermore, since restricting the rate of engine speed increase also minimizes shifting inertia loss, this control achieves linear changes in G and helps to reduce the so-called rubber band feeling of a CVT. As a result, mating this turbocharged engine with a CVT enables the CVT shifting control to optimize both boost pressure response and driving force response.

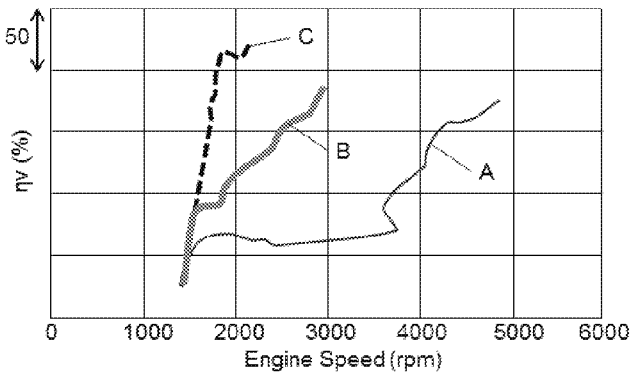

Figure 30. Differences in in-cylinder airflow history

Figure 31 shows the acceleration curves from 40 km/h with the CVT and manual transmission. Although the increase in acceleration is slightly delayed with the CVT by the amount of inertia loss during shifting, the vehicle achieves an acceleration feeling in accordance with the intention of the driver, which is one of the main characteristics of a CVT. By optimizing the shifting control (i.e., the amount and speed of shifting) in accordance with driver operation (i.e., the amount and speed of accelerator depression), the CVT achieves the same linear acceleration as a manual transmission under gradual acceleration, as well as linear and high-peak G response under rapid acceleration. The result is smooth acceleration that does not convey a sensation of turbocharger lag to the driver.

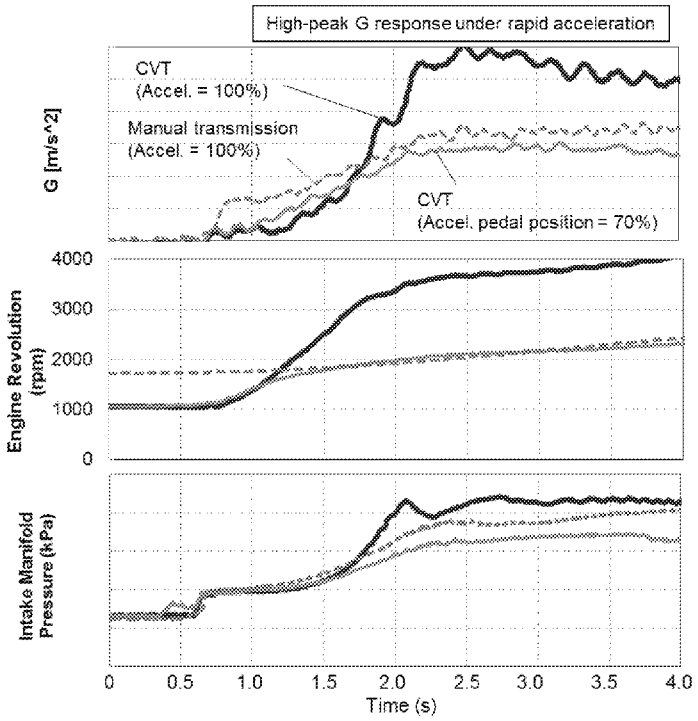

Figure 31. Comparison of CVT and manual transmission

Figure 32 shows the vehicle longitudinal G curves from a standing start of vehicles equipped with a dual clutch transmission (DCT) or CVT. The DCT is short-geared with 10% of the total gear ratio. Compared to the delayed start response created by the clutch engagement of the DCT, the CVT has the better initial starting performance due to the torque amplification function of the torque converter. In addition, although the G in the middle region is slightly lower than the DCT due to torque converter loss, its torque amplification function gives the CVT roughly the same peak G as the DCT with the shorter total gear ratio. Considering the overall acceleration event, a smooth and linear feeling can be achieved with the CVT.

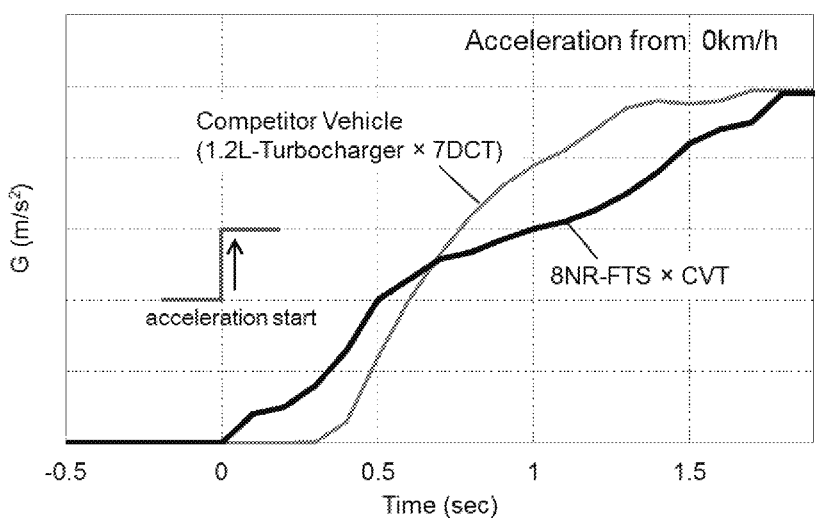

Figure 32. Comparison of CVT and DCT

In addition to the normal operating mode, the CVT is also equipped with a sport mode. In normal mode, the CVT achieves linear acceleration using low-end torque, as described above. In sport mode, the G response is increased by changing the engine torque with shifting control, achieving a direct acceleration (Fig. 33). This faster G response is accomplished by increasing the boost pressure response by raising the engine speed during lock-up, and by increasing the engine torque demand for a given accelerator position. Furthermore, engine speed is raised to improve the boost pressure response, and the shifting control is performed more quickly than in normal mode, further enhancing G response. Through these measures, sport mode achieves a more direct feeling of acceleration and makes the vehicle even more enjoyable to drive.
In conclusion, integrating this turbocharged engine with the optimum CVT shifting control minimizes the rubber band feeling and achieves exciting new dynamic performance.

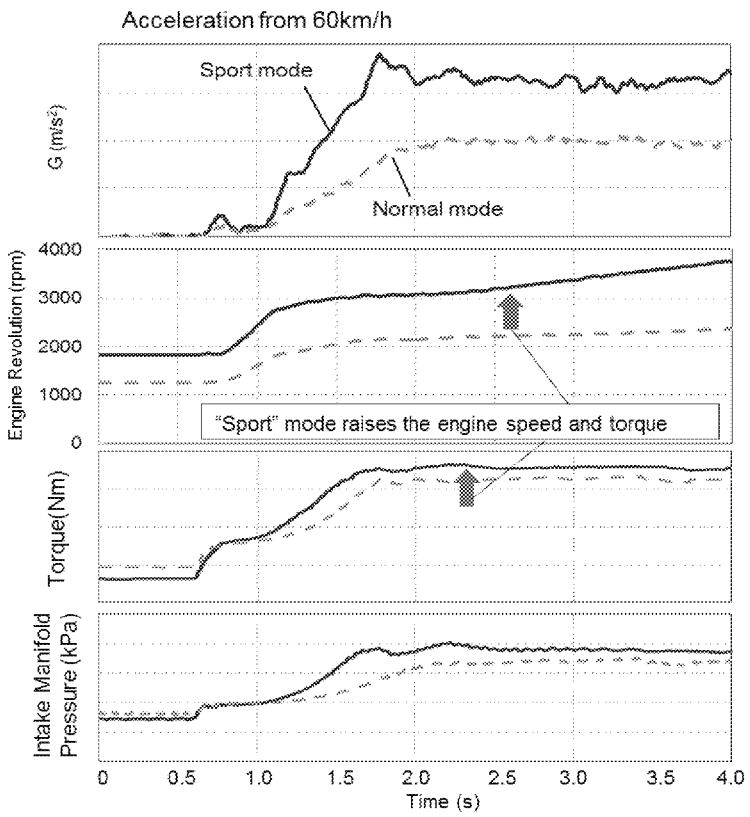

Figure 33. The Effects of “Sport” mode

When climbing a gradient or towing in hot weather, the coolant and intake temperatures become hot. The subsequent retardation control to prevent knocking results in a higher exhaust temperature and greatly increases the amount of heat transferred from the coolant of the cylinder head with integrated exhaust manifold. This situation may lead to overheating. As a countermeasure, cooperative control is carried out with the CVT to shift the engine operating line to the high engine speed side, increase the flow of coolant within the engine, and lower the outlet coolant temperature. Furthermore, adopting an operating point with low cooling loss restricts the increase in coolant temperature and minimizes the increase in radiator and electric fan capacity, while ensuring dynamic performance.

7. Improvement of Cold Start Combustion Performance

Since this engine does not use port injection, the promotion of fuel atomization and A/F mixing is an issue under extremely cold temperatures. This was addressed by actively applying a multiple injection strategy in the same way as the engine fuel economy improvements described above. Figure 34 shows a schematic view of the multiple injections when starting the engine under extremely cold temperatures. Each injection in the intake stroke is used to form a lean mixture in the combustion chamber and the injection in the compression stroke is used to form a combustible gas mixture around the plug. The spray length is restricted by splitting the injections in the intake stroke, thereby minimizing wetting of the fuel on the bore. As a result, this engine achieves a shorter start time compared to the extremely low-temperature start performance of the conventional port injection.

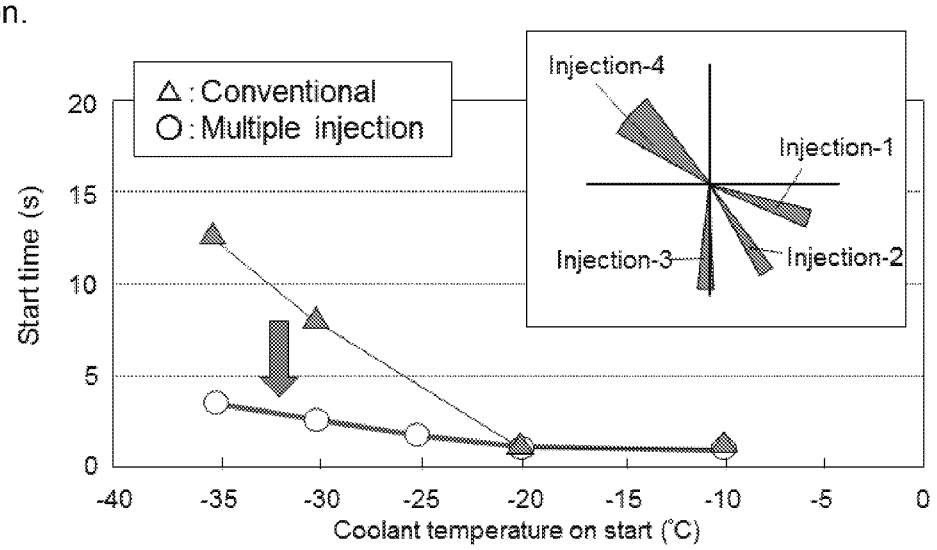

Figure 34. Cold start injection strategy and cold start time

8. Conclusions

This paper has described the hardware and software characteristics of new Toyota 8NR-FTS 1.2L ESTEC D-4T engine. The main points of this engine can be summarized as follows.

- This engine achieves high-speed combustion without port injection by intensifying the intake flow and in-cylinder turbulence, and by adopting a multiple injection strategy per combustion cycle.
- Maximum torque is generated from 1,500 rpm by adopting a single-scroll turbocharger, small exhaust cam event angle, and scavenging control.
- Lambda = 1 area is expanded by cooling the exhaust gas in a cylinder head with integrated exhaust manifold.
- Class-leading vehicle fuel economy is achieved by adopting a shock-free and smooth engine stop control that allows immediate engine re-start in the DI compression stroke, improving the combustion characteristics of the engine, adopting a high-geared shifting control, and so on.
- Mating this engine with CVT shifting control achieves both sporty dynamic performance and excellent fuel economy.

9. References

1. Izumi, W., Takashi, K., Koichi, Y., Teru, O., "The New Toyota 2.0-Liter Inline 4-Cylinder ESTEC D-4ST Engine - Turbocharged Direct Injection Gasoline Engine -," 23rd Aachen Colloquium Automobile and Engine Technology, Aachen 2014.
2. Mitani, S., Hashimoto, S., Nomura, H., Shimizu, R. et al., "New Combustion Concept for Turbocharged Gasoline Direct-Injection Engines," SAE Technical Paper 2014-01-1210, 2014, doi:10.4271/2014-01-1210.
3. Guido, V., Christian, E., Norbert, M., Fritz, K., "The New 2.0l Turbo Engine from the Mercedes-Benz 4-Cylinder Engine Family," 21st Aachen Colloquium Automobile and Engine Technology, Aachen 2012.
4. Rainer, W., Ralf, B., Joachim, B., Rolf, D., et al., "The New 2.0L TFSI with the Audi Valvelift System for the Audi A4 – The Next Generation of the Audi TFSI Technology," 17th Aachen Colloquium Automobile and Engine Technology, Aachen 2008.
5. Okada, Y., Miyashita, S., Izumi, Y., and Hayakawa, Y., "Study of Low-Speed Pre-Ignition in Boosted Spark Ignition Engine," SAE Int. J. Engines 7(2):584-594, 2014, doi:10.4271/2014-01-1218.
6. Philipp, A., Jürgen, D., Matthias, T., Jens, E., et al., "Effect of Fuel and Combustion System on the Pre-Ignition of Boosted SI engines," 34th International Motor Symposium, Vienna, 2013.